

Electronic Supplementary Information

Newly Design Porous/Sponge Red Phosphorus@Graphene and Highly Conductive Ni₂P Electrode for Asymmetric Solid State Supercapacitive Device With Excellent Performance

Nazish Parveen,¹ Muhammed Hilal,² and Jeong In Han*²

¹Department of Chemistry, College of Science, King Faisal University, Al-Ahsa 31982, Saudi Arabia

²Flexible display and printed electronic lab, Department of Chemical and Biochemical Engineering, Dongguk University-Seoul, 04620 Seoul, Republic of Korea

Table. S1 Performance comparison of the nickel phosphide-based electrode materials in three-electrode configuration with previously published results.

S. No.	Electrode material	Electrolyte	Current density (Ag ⁻¹)	Specific capacitance (Fg ⁻¹)	Retention %	No of cycles	Ref.
1	Ni ₂ P	2.0M LiOH	1	418			1
2	Ni-coated Ni ₂ P	2.0M LiOH	1	581	92.3	3,000	1
3	Ni ₂ P nano belt	0.5M H ₂ SO ₄	0.625	1074	86.7	3000	2
4	Ni ₂ P/Ni ₁₂ P ₅	2M KOH	1	1325.7	81	20,000	3
5	Ni-P	2.0 M KOH	1	1338.7	71.4	1,000	4
6	Ni ₂ P	2.0 M KOH	1	843.3	100	1000	5
7	Au/Ni ₁₂ P ₅	2.0 M KOH	0.2	806.1	91.0	1,000	6
8	Ni ₂ P/rGO	2.0 M KOH	1	2354	100	2,500	7
9	Ni ₂ P NS/NF	6.0 M KOH	2.5	3496	61.0	5,000	8
10	Ni ₂ P	2.0 M KOH	1	600	82.5	1,000	9
11	Ni ₂ P@5%GR	3 M KOH	1	672.4	30	2000	10
12	Ni ₂ P nano particle	3M KOH	1	668.7	--	--	11
13	Ni ₂ P	2M KOH	1	1526.6	88	2,500	Present work
14	Ni ₂ p	2M KOH	1	980	--	--	Present work

Picture of the rP@rGO foam



Figure. S1 Picture of red phosphorus@graphene foam.

Assembled asymmetric supercapacitive device

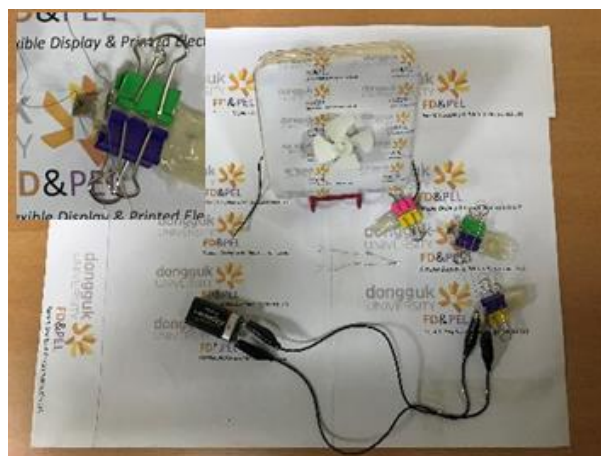


Figure. S2 Picture of assembled asymmetric supercapacitive device.

SEM, TEM, and HRTEM images of the B-rGO

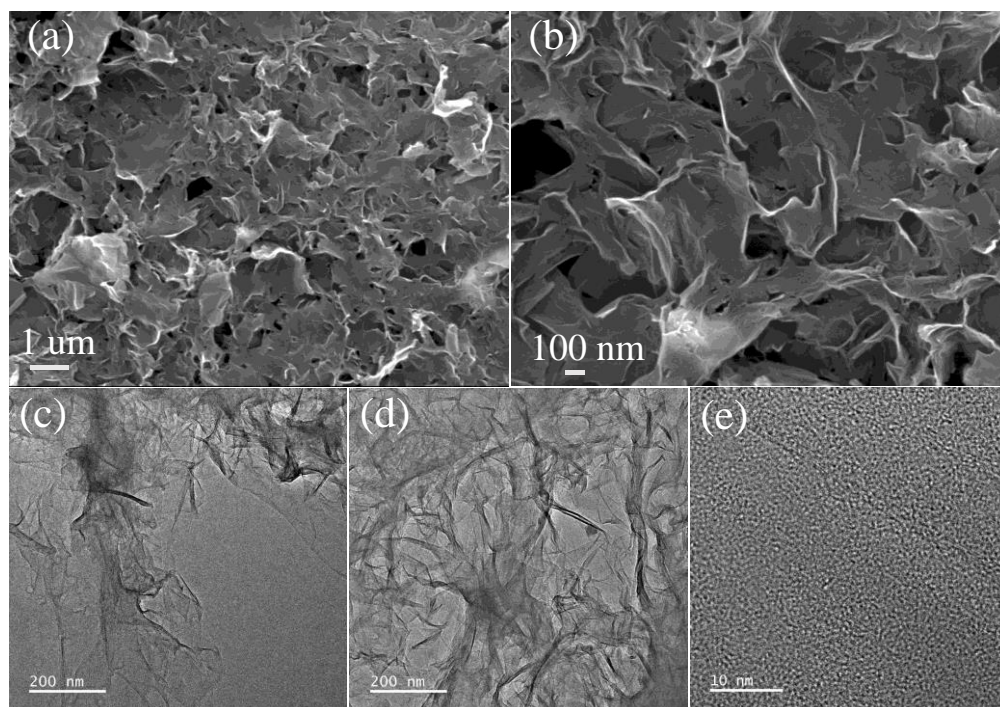


Figure. S3 (a-b) SEM images (c-d) TEM image and (e) HRTEM images of the B-rGO.

Survey spectra of the rP@rGO

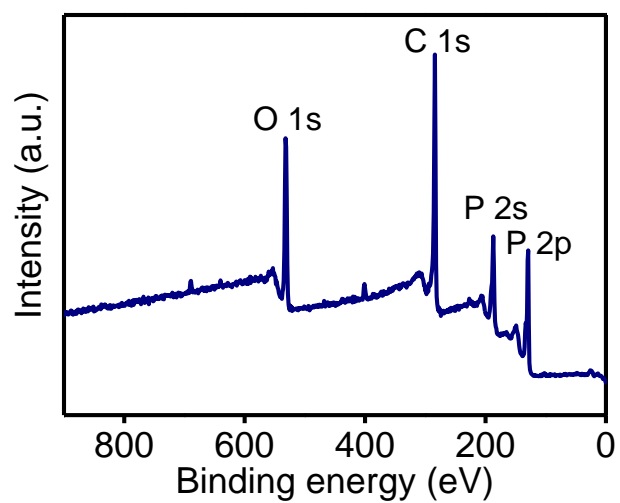


Figure. S4 XPS survey spectra of the rP@rGO.

O 1s spectra of the rP@rGO

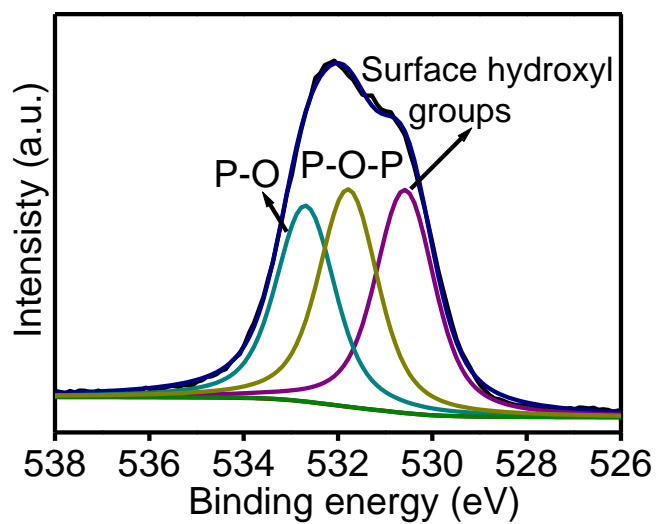


Figure. S5 O 1s spectra of the rP@rGO.

SEM and mapping images of the Ni₂P-1

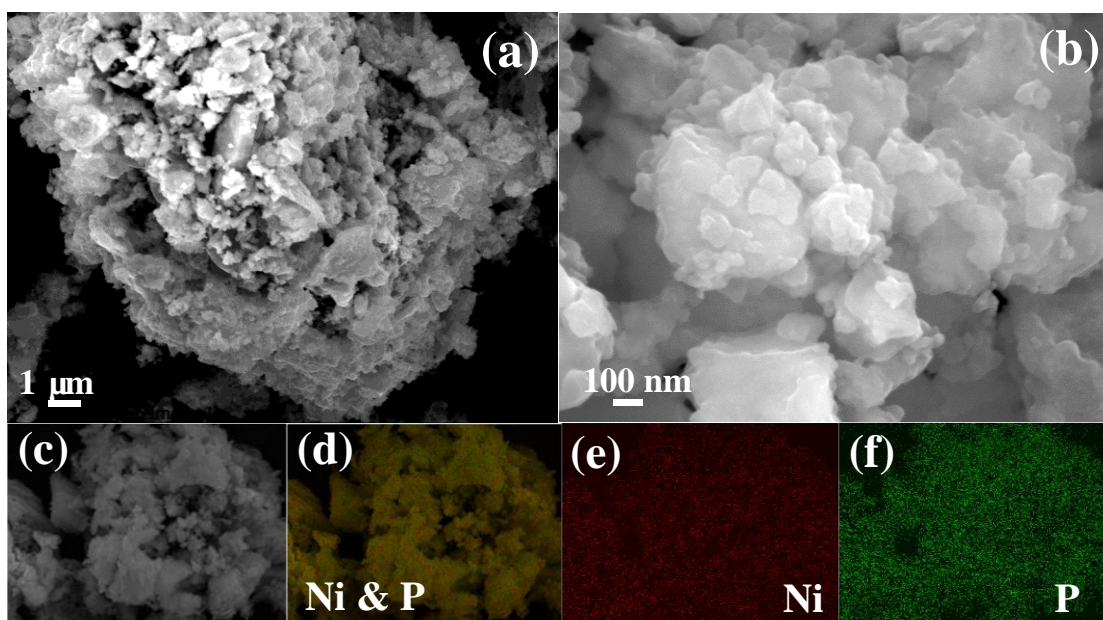


Figure S6. (a and b) SEM images, and (c-f) corresponding elemental mapping of the Ni₂P-1.

XPS spectra of Ni₂P-2

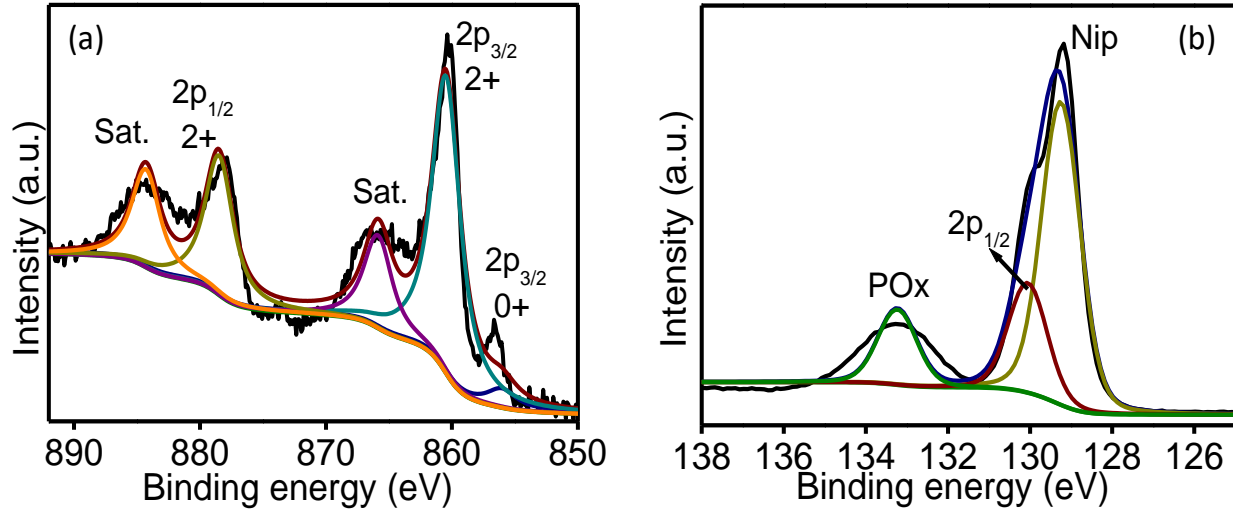


Figure S7. High magnification XPS spectra of Ni₂P (a) Ni and (b) P.

To estimate the specific capacitance of the as prepared positive and negative electrode inside the half-cell assembly the following equation were used.^{3,5}

$$C = \frac{I dt}{m dV} \quad (S1)$$

Where C is the specific capacitance (F/g), I is the applied current, t is the discharge time, m represent the mass of the active materials over the surface of the current collector, and dV is the applied potential window.

To estimate the specific capacitance of the assembled asymmetric supercapacitor gadget the following equation are used.^{3,5}

$$C = \frac{I dt}{m dV} \quad (S2)$$

Where C is the specific capacitance (F/g), I is the applied current, t is the discharging time, m is active mass loading over the surface of the current collector, and dV is the applied potential

window.

Whereas the power density and energy density were estimated from the following equation:⁵

$$E = \frac{1}{2}CV^2 \quad (\text{S3})$$

$$P = \frac{E}{t} \quad (\text{S4})$$

Where C is the specific capacitance, V is the applied potential window and t is the discharging time of the device.

The CV profile of all the Ni₂P electrodes

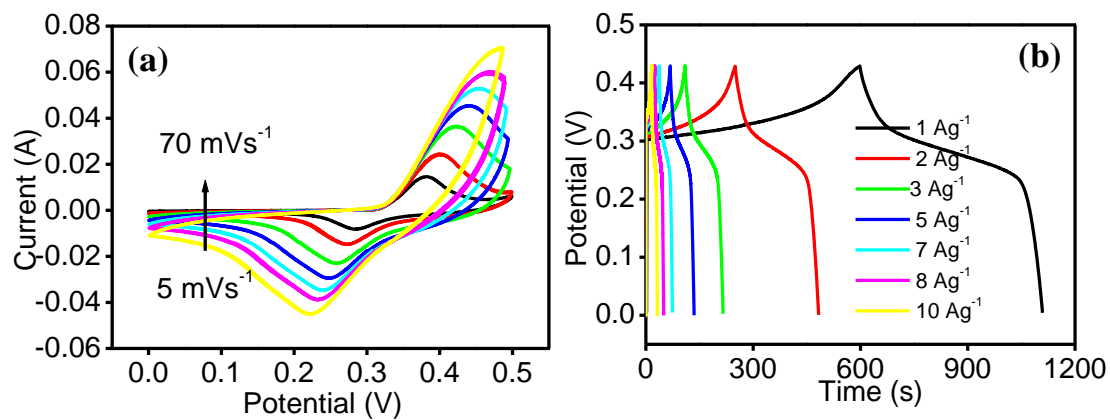


Figure S8. The CV (a) and CD (b) profile of Ni₂P-1 electrode.

Picture of the assembled device illumination of the LED light

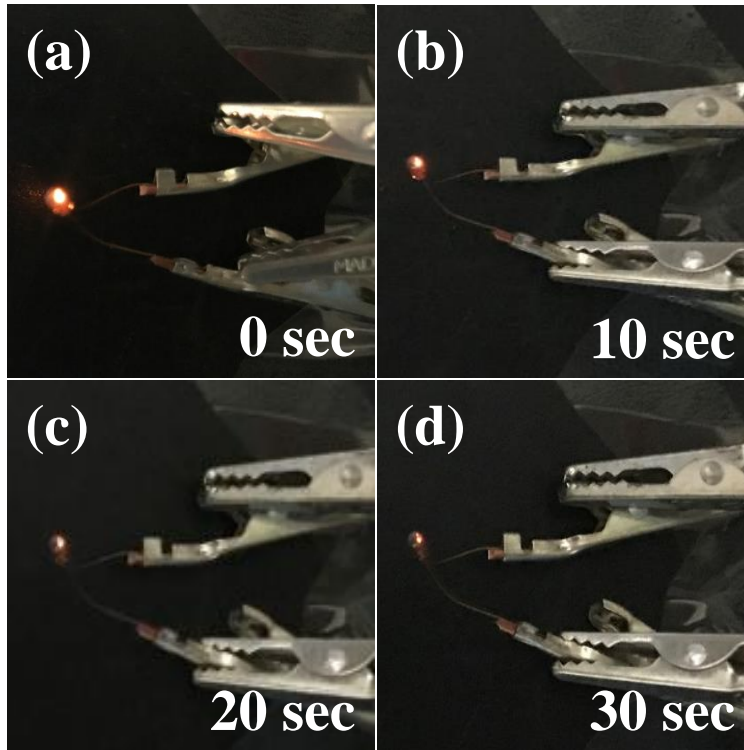


Figure S9. (a-d) Picture of the assembled device illumination of the LED light.

Picture of the assembled device and fan powered by the assembled device

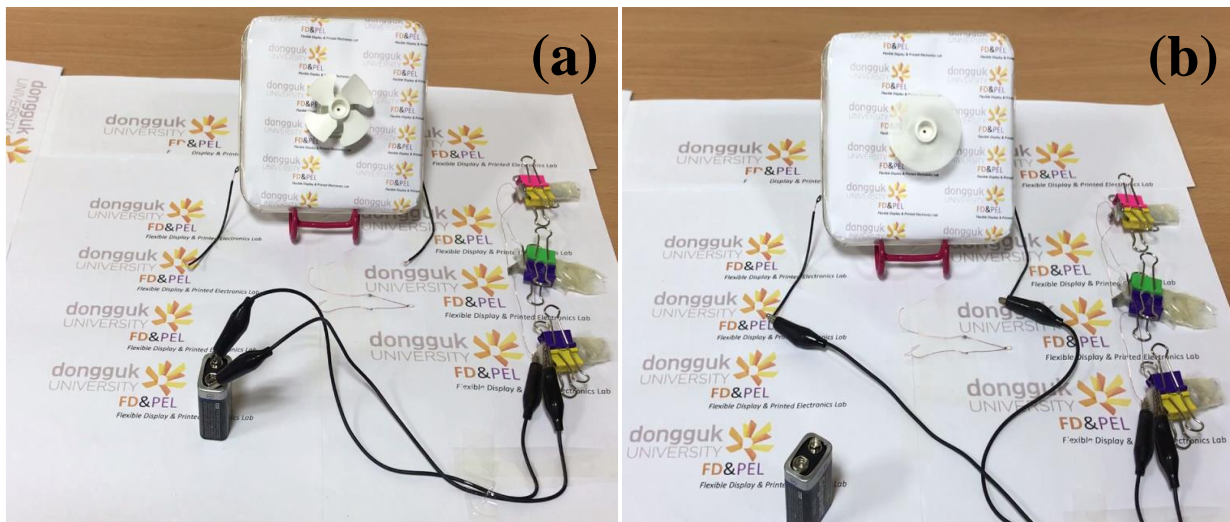


Figure S10. Picture of the assembled device and fan powered by the assembled device.

References

1. Y. Lu, J. K. Liu, X. Y. Liu, S. Huang, T. Q. Wang, X. I. Wang, C. D. Gu, J. P. Tu and S. X. Mao, Facile synthesis of Ni-coated Ni₂P for supercapacitor applications, *Cryst Eng Comm*, 2013, 15, 7071.
2. Y. Jin a, C. Zhao, L. Wang, Q. Jiang, C. Ji, X. He, Preparation of mesoporous Ni₂P nanobelts with high performance for electrocatalytic hydrogen evolution and supercapacitor, *international journal of hydrogen energy* 2018,43, 3697-3704.
3. S. Xie, J. Go, Facile synthesis of Ni₂P/Ni₁₂P₅ composite as long-life electrode material for hybrid supercapacitor, *Journal of Alloys and Compounds*, 2017, 713, 10-17.
4. D. Wang, L. B. Kong, M. Liu, W. B. Zhang, Y. C. Luo, L. Kang, Amorphous Ni–P materials for high performance pseudocapacitors, *Journal of Power Sources*, 2015, 274, 1107-1113.
5. D. Wang, L. B. Kong, M. C. Liu, Y. C. Luo, L. Kang, An Approach to Preparing Ni–P with Different Phases for Use as Supercapacitor Electrode Materials, *Chem. Eur.J.*2015, 21,17897 –17903
6. S. Duan and R. Wang, Au/Ni₁₂P₅ core/shell nanocrystals from bimetallic heterostructures: in situ synthesis, evolution and supercapacitor properties, *NPG Asia Materials*, 2014, 6, 122.
7. C. An, Y. Wang, Y. Wang, G. Liu, L. Li, F. Qiu, Y. Xu, L. Jiao and H. Yuana, Facile synthesis and superior supercapacitor performances of Ni₂P/rGO nanoparticles, *RSC Adv.*, 2013, 3, 4628-4633
8. K. Zhou, W. Zhou, L. Yang, J. Lu, S. Cheng, W. Mai, Z. Tang, L. Li, S. Chen, Ultrahigh-Performance Pseudocapacitor Electrodes Based on Transition Metal Phosphide

Nanosheets Array via Phosphorization: A General and Effective Approach, *Advanced Functional Materials*, 2015, 25, 7530-7538.

9. M. C. Liu, Y. M. Hu, W. Y. An, Y. X. Hu, L. Y. Niu, L. B. Kong, L. Kang, Construction of high electrical conductive nickel phosphide alloys with controllable crystalline phase for advanced energy storage, *Electrochimica Acta*, 2017, 232, 387–395
10. W. Du, S. Wei, K. Zhou, J. Guo, H. Pang, X. Qian, One-step synthesis and graphene-modification to achieve nickel phosphide nanoparticles with electrochemical properties suitable for supercapacitors, *Materials Research Bulletin*, 2015, 61, 333–339.
11. W. Du, R. Kang, P. Geng, X. D. Li, Q. Tian, H. Pang, New asymmetric and symmetric supercapacitor cells based on nickel phosphide nanoparticles, *Materials Chemistry and Physics*, 2015, 165, 207-214.